HIGH TEMPERATURE TENSILE PROPERTIES AND FATIGUE BEHAVIOR OF A MELT-INFILTRATED SIC/SIC COMPOSITE

Sreeramesh Kalluri*, Anthony M. Calomino#, and David N. Brewer@

High temperature fatigue behavior of a woven, SiC/SiC ceramic matrix composite (CMC) was investigated in air at two temperatures. The reinforcement for the CMC consisted of 5HS Sylramic ™ fabric with a $[0°/90°]_{4S}$ lay-up. The SiC matrix material was infiltrated into the fiber-preform with a slurry-cast, melt-infiltration process. Tensile and fatigue test specimens were machined from the CMC plates. Initially tensile tests were conducted to obtain the average values of tensile properties at 1038 and 1204°C. Subsequently, low-cycle fatigue (LCF) tests with zero and two-hour hold-times at the maximum stress were conducted at the same two temperatures. Fatigue life data generated in the LCF tests were used to determine the geometric mean fatigue lives. In this paper, the tensile behavior and the fatigue durability of the CMC determined under different loading conditions are documented. In addition, reductions observed in the cyclic lives of the composite due to the two-hour hold-time at maximum tensile stress are discussed.

INTRODUCTION

Ceramic matrix composites (CMCs) are under consideration as combustor and nozzle component materials for advanced gas turbine engines [1]. High temperature capability in conjunction with the high specific strength makes the CMCs very attractive candidates in comparison to conventional metallic alloys. In order to design gas turbine engine components with CMCs, the mechanical properties of these materials (for example, tensile and creep) and the high temperature durability of these materials under cyclic loading conditions (for example, fatigue and creep-fatigue) need to be characterized in a reliable manner.

In this investigation, the tensile and fatigue properties of a woven, SiC/SiC CMC at two different temperatures were characterized. The tensile properties and fatigue lives generated with and without hold times on multiple test specimens were utilized to document both the average behavior of the material and the variability associated with each of the characterized properties.

*Ohio Aerospace Institute, NASA Glenn Research Center, 21000 Brookpark Road, Mail Stop: 49- 7, Brook Park, Ohio 44135, USA. #NASA Glenn Research Center, Brook Park, Ohio, USA. @US Army Research Laboratory, NASA Glenn Research Center, Brook Park, Ohio, USA.

MATERIAL AND TEST SPECIMENS

Reinforcement for the SiC/SiC composite consisted of Sylramic™ fiber woven to a five harness satin weave configuration with a $[0°/90°]_{4S}$ lay-up for the fiber-preform. The SiC matrix material was infiltrated into the fiber-preform with a slurry-cast, melt-infiltration (MI) process. Nominal dimensions of the as-fabricated (in September 1999) CMC plates were as follows: 229 mm length, 152mm width, and 2 mm thickness. Tensile and fatigue test specimens (Fig. 1) were machined from the as-fabricated CMC plates. Overall length of the test specimen was 152 mm, with nominal test section width and length of 10.2 and 28 mm, respectively. Verrilli et al. [2] and Unal [3] utilized test specimens with similar geometries to investigate the creep-rupture behavior and to characterize the tensile and fatigue behaviors of CMCs, respectively.

EXPERIMENTAL DETAILS

Tensile tests and fatigue tests (both with no hold-time and a 2 hr. hold-time at the maximum load) were conducted at 1038 and 1204°C. Test specimens were heated to the required test temperature within an inductively heated, monolithic SiC susceptor [2]. Temperature of each test specimen was both controlled and monitored with two R-type beaded thermocouples located inside the susceptor in the vicinity of the test specimen. Test specimens were loaded in test frames equipped with water-cooled, hydraulically activated, wedge grips. Test frames were aligned with strain-gaged bars such that the maximum bending strain produced in the alignment bar was less than 10% at a tensile load of 4.44 kN. Displacement within the test section of each specimen was measured with a 12.7 mm gage section, air-cooled extensometer equipped with alumina probes. All the tensile tests were conducted in displacement-control, whereas all the fatigue tests (both with and without hold-time) were conducted in load-control. In continuous cycling fatigue tests, triangular waveforms with an R (minimum load/maximum load) value of 0.05 and a frequency of 0.33 Hz were used. In the case of fatigue tests with hold-time, a two-hour dwell period was imposed at the maximum load in each cycle. Failure in all the fatigue tests was defined as separation of the test specimen into two pieces.

RESULTS AND DISCUSSION

Tensile Properties

In order to assess variability in the tensile properties multiple test specimens were used to generate the data at 1038 and 1204°C. A total of six specimens were tested at 1038°C, whereas a total of 24 specimens were tested at 1204°C. Data obtained from each tensile test were used to determine the elastic modulus (E), proportional limit strength (PLS: 0.005% offset), in-plane tensile strength (ITS), and strain to failure (SF) for that specimen. The average tensile properties of MI SiC/SiC composite at 1038 and 1204°C are listed in Table 1. In order to compare both the average values and the variability associated with each tensile property, these tensile properties are also shown in the form of bar charts in Figs. 2 to 5. In these figures, the error bars represent 95% confidence intervals and are obtained by doubling the standard deviation associated with each tensile property.

TABLE 1 Average Tensile Properties of MI SiC/SiC Composite at 1038 and 1204°C

Temperature (°C)	Number of Tests	E (GPa)	PLS (MPa)	ITS (MPa)	SF (%)
1038	6	209	168	325	0.44
1204	24	182	166	307	0.46

Both the elastic modulus and in-plane tensile strength of MI SiC/SiC composite decreased as the temperature increased from 1038 to 1204°C. No significant changes were observed in the proportional limit strength and strain to failure of the composite with the increase in temperature. Note that the lengths of error bars for elastic modulus and strain to failure at 1038 and 1204°C are similar and the error bar lengths for in-plane tensile and proportional limit strengths at these two temperatures are not significantly different (Figs. 2 to 5). Since six specimens were tested at 1038°C and 24 at 1204°C, these observations in the lengths of error bars suggest that at a given temperature six tensile tests are sufficient to obtain the average tensile properties and reasonable estimates of variability associated with each of those properties. However, six tensile tests will not to be sufficient to characterize the distributions associated with the tensile properties. To illustrate this issue, the in-plane tensile strengths observed in the all the tensile tests performed in this investigation are plotted in Figure 6. The probability of failure associated with each datum was estimated with the median rank method. At 1204°C, where 24 tests were conducted, in-plane tensile strength data appear to fall along a straight line representing a normal distribution (Fig. 6). However, such a trend is not exhibited by the in-plane tensile strength data at 1038°C, where only six tests were performed.

Fatigue Behavior

Fatigue tests were conducted with no hold-time and a hold-time of 2 hr. at the maximum load at 1038 and 1204°C. Three tests were performed at each test condition to obtain the representative fatigue life associated with that condition. A maximum stress of 179 MPa was selected for all the fatigue tests. For each test condition, geometric mean fatigue life was calculated from the three fatigue lives obtained in the experiments. The geometric mean fatigue lives for the four test conditions are plotted in Fig. 7. The error bar associated with each fatigue test condition represents the degree of scatter observed in cyclic lives for that condition.

For no hold-time and 2 hr. hold-time fatigue loading conditions, the geometric mean fatigue lives at 1204°C were lower than the corresponding cyclic lives at 1038°C (Fig. 7). Since the applied maximum stress of 179 MPa used in the fatigue tests constitutes about 55% and 58% of the in-plane tensile strength at 1038 and 1204°C, respectively, the reduction in fatigue life at 1204°C is likely due to enhanced cyclic damage accumulation mechanisms such as oxidation. Geometric mean fatigue life decreased by an order of magnitude or more with the introduction of two hr. hold-time at both the temperatures. The reduction in cyclic life due to hold-time was significantly greater (more than two orders of magnitude) at 1204°C than at 1038°C (Fig. 7). The applied maximum stress was greater than the average proportional limit strengths at both the temperatures (Table 1). As a result, matrix cracks formed during the initial loading could oxidize during the two hr. hold-period and with each subsequent cycle of loading such a mechanism could either produce more oxidized cracks or increase the lengths and oxide contents within existing cracks in the composite, which could result in lower cyclic life. This mechanism would be more pronounced at 1204°C than at 1038°C due to enhanced diffusion rates of oxygen through the cracks at the higher temperature during the hold-period. Note that in the absence of the hold-period, the reduction in fatigue life at 1204°C was not as dramatic (Fig. 7). Note that the scatter in fatigue lives (as seen from the error bars in Fig. 7) at 1038°C is higher than that at 1204°C. Since the number of tests conducted at all the test conditions was identical, this observation suggests that different fatigue damage mechanisms may be operating at the two temperatures. Interrupted fatigue tests in air as well as fatigue tests in inert environments (for example, argon or vacuum) are necessary to identify the prevailing damage mechanisms.

CONCLUDING REMARKS

High temperature tensile properties and fatigue behavior of a melt-infiltrated, SiC/SiC composite were characterized at 1038 and 1204°C by conducting multiple tests per test condition. Average values of elastic modulus, proportional limit strength, in-plane tensile strength, and strain to failure and the variation within each of these properties were evaluated for both the temperatures. Geometric mean fatigue lives were determined for test conditions with no hold-time and two-hour hold-time at the maximum load. Fatigue durability of the composite decreased with increasing temperature and hold-time. Potential reasons for the observed reductions in the cyclic lives of the composite were discussed.

ACKNOWLEDGEMENTS

Financial Support for this work was obtained from NASA Glenn Research Center, Brook Park, Ohio under cooperative agreement NCC-3-618 through the Ultra Efficient Engine Technology Program. Authors are grateful to Mr. John D. Zima and Mr. William L. Brown for conducting the tensile and fatigue tests at NASA Glenn Research Center.

REFERENCES

(1) Shaw, R. J., Koops, L., and Hines, R., *Progress Toward Meeting the Propulsion Technology Challenges for a 21st Century High-Speed Civil Transport*, NASA TM 113161, ISABE-97-7045, XIII International Symposium on Air Breathing Engines, Sponsored by American Institute of Aeronautics and Astronautics, Chattanooga, Tennessee, September 8-12, 1997.

(2) Verrilli, M. J., Calomino, A. M., and Brewer, D. N., Creep-Rupture Behavior of a Nicalon/SiC Composite, *Thermal and Mechanical Test Methods and Behavior of Continuous-Fiber Ceramic Composites, ASTM STP 1309*, M. G. Jenkins, S. T. Gonczy, E. Lara-Curzio, N. E. Ashbaugh, and L. P. Zawada, Editors, American Society for Testing Materials, pp. 158-175, 1997.

(3) Unal, O., Tensile and Fatigue Behavior of a Silicon Carbide/Silicon Carbide Composite at 1300°C, *Thermal and Mechanical Test Methods and Behavior of Continuous-Fiber Ceramic Composites, ASTM STP 1309*, M. G. Jenkins, S. T. Gonczy, E. Lara-Curzio, N. E. Ashbaugh, and L. P. Zawada, Editors, American Society for Testing Materials, pp. 113-127, 1997.

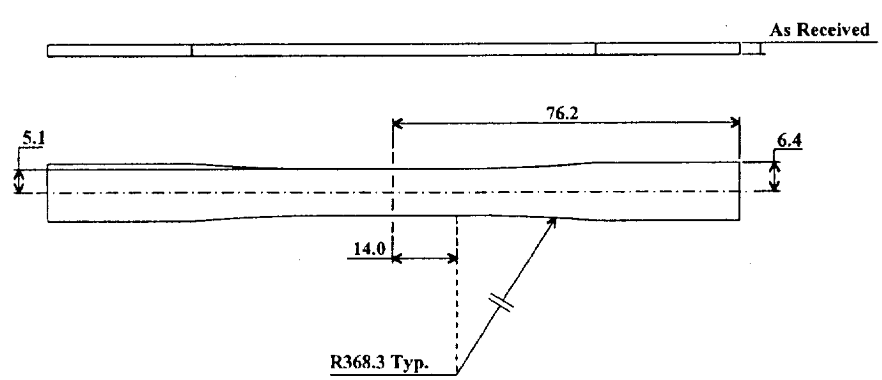

FIGURE 1 Geometry of the MI SiC/SiC Test Specimen Used in Tensile and Fatigue Tests. All the dimensions are in mm.

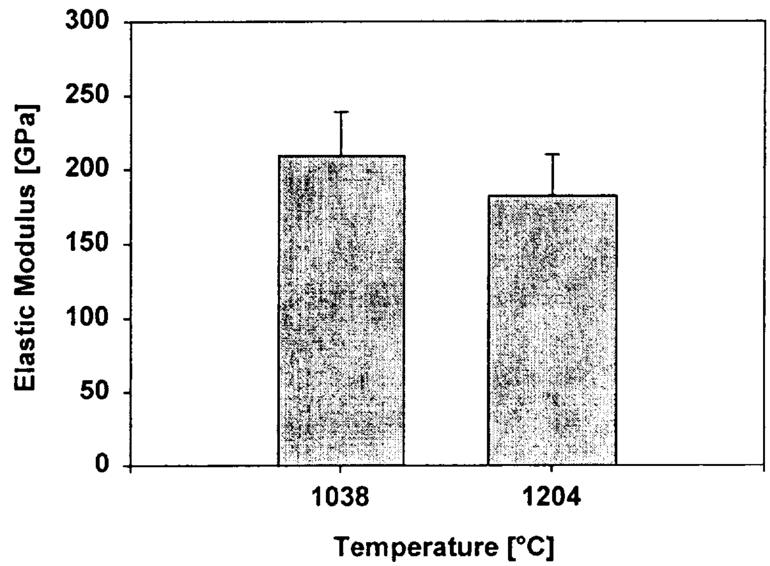

FIGURE 2 Average In-Plane Elastic Moduli and 95% Confidence Intervals for the MI SiC/SiC Composite.

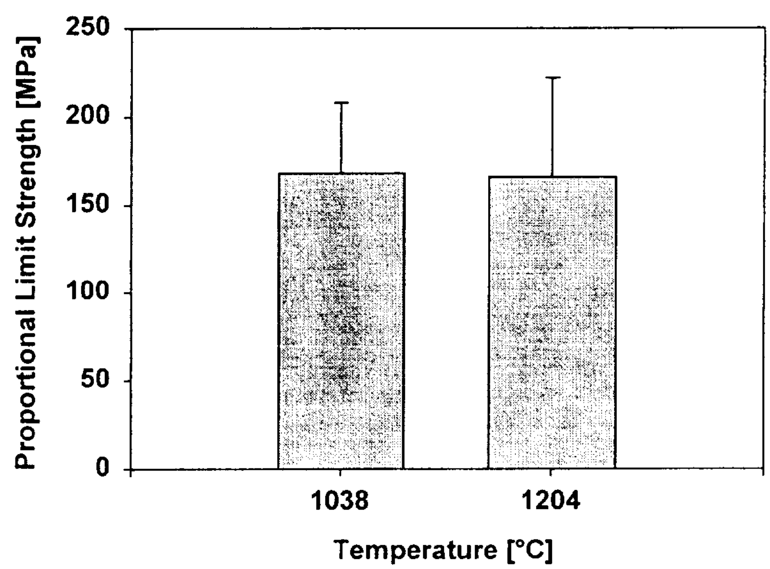

FIGURE 3 Average In-Plane Proportional Limit Strengths and 95% Confidence Intervals for the MI SiC/SiC Composite.

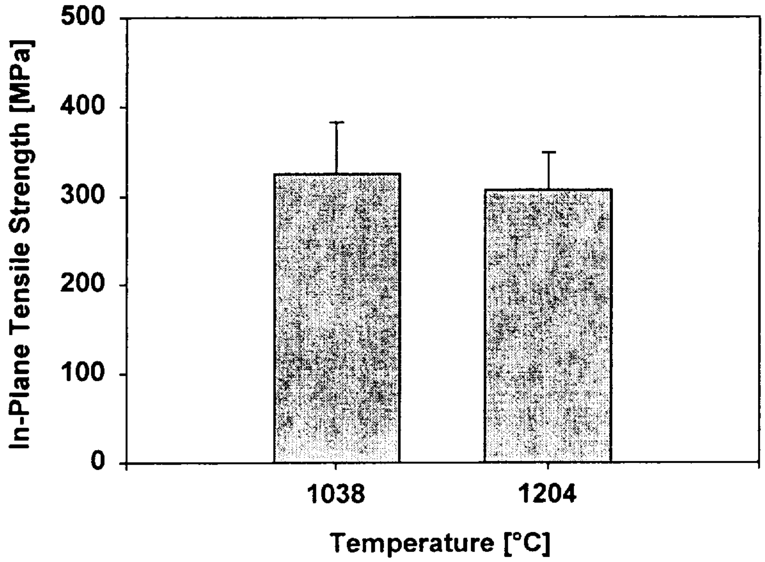

FIGURE 4 Average In-Plane Tensile Strengths and 95% Confidence Intervals for the MI SiC/SiC Composite.

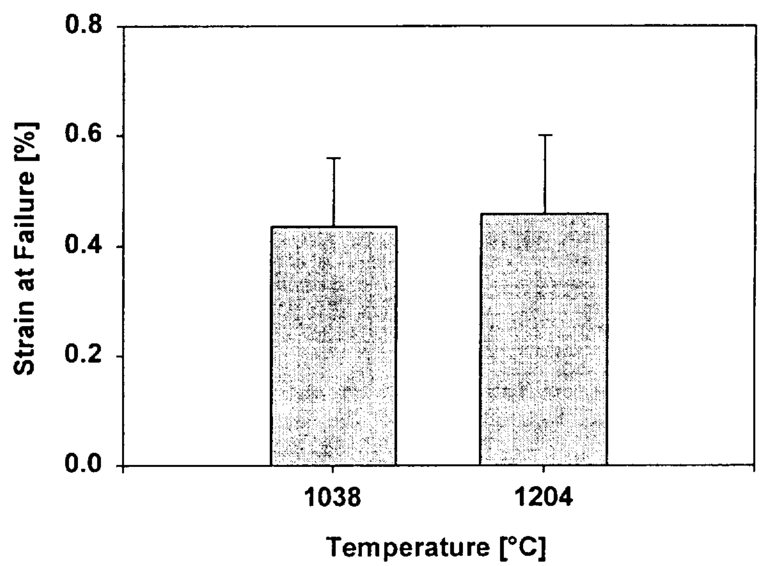

FIGURE 5 Average Strains to Failure and 95% Confidence Intervals for the MI SiC/SiC Composite.

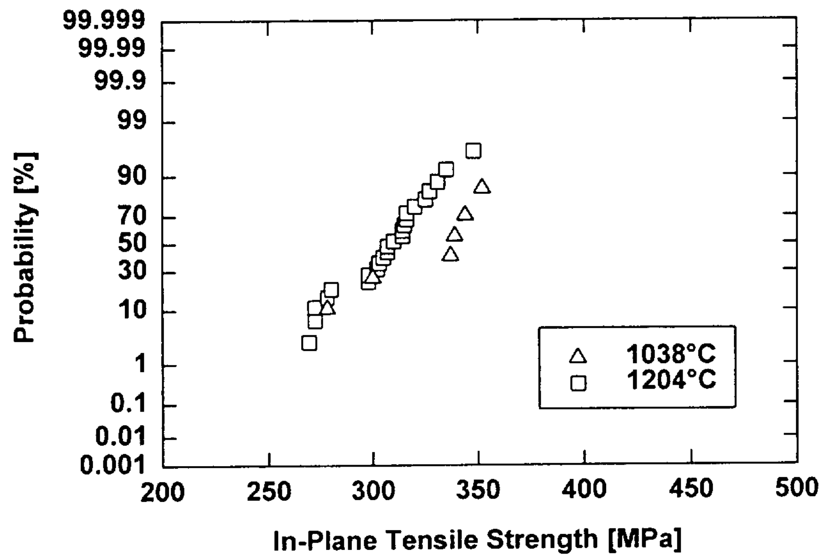

FIGURE 6 Distributions of the In-Plane Tensile Strengths for the MI SiC/SiC Composite.

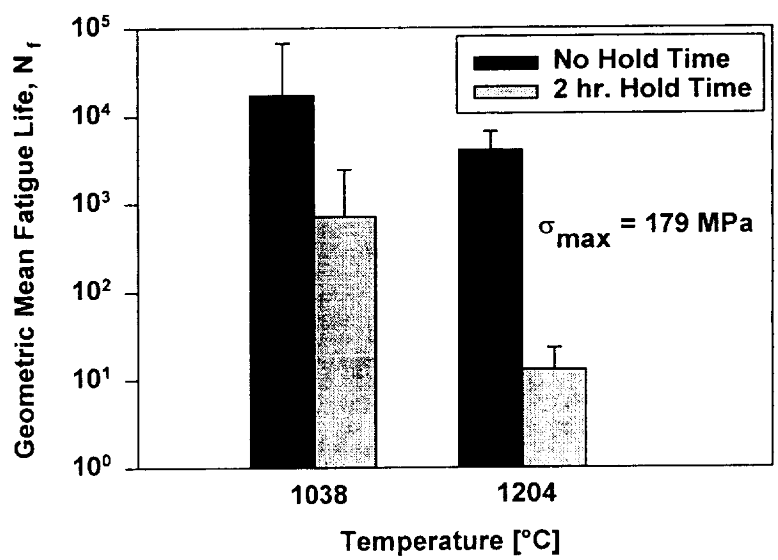

FIGURE 7 Fatigue Lives with and without Hold- Times for the MI SiC/SiC Composite.